Peripheral nerve involvement in multiple sclerosis

Demonstration by magnetic resonance neurography

Original research article

Johann M.E. Jende, MD,[1*] Gesa H. Hauck, MD,[1,2*] Ricarda Diem, MD,[3] Markus Weiler, MD,[3] Sabine Heiland, PhD,[1,4] Brigitte Wildemann, MD,[3] Mirjam Korporal-Kuhnke, MD,[3] Wolfgang Wick, MD,[3] John M. Hayes, BA[5] Johannes Pfaff, MD,[1] Mirko Pham, MD,[1,6] Martin Bendszus, MD,[1] Jennifer Kollmer, MD[1]

1 Department of Neuroradiology, Heidelberg University Hospital, Heidelberg, Germany
2 Department of Radiology, Hannover Medical School, Hannover, Germany
3 Department of Neurology, Heidelberg University Hospital, Heidelberg, Germany
4 Division of Experimental Radiology, Department of Neuroradiology, Heidelberg, Germany
5 Department of Neurology, University of Michigan, Ann Arbor, USA
6 Department of Neuroradiology, Würzburg University Hospital, Würzburg, Germany

Corresponding Authors:
Jennifer Kollmer, MD
Department of Neuroradiology
Heidelberg University Hospital
Im Neuenheimer Feld 400
D-69120 Heidelberg
Germany
Phone: +49 6221 5638305
Fax: +49 6221 564673
Email: jennifer.kollmer@med.uni-heidelberg.de

* Johann M.E. Jende and Gesa H. Hauck contributed equally

Number of characters in the title: 50
Number of characters in the running head: 47
Number of words in the Abstract: 256
Number of words in the Introduction: 277
Number of words in the Discussion: 1228
Number of words in the body of the manuscript: 4072
Number of figures: 4 (color figures: 0)
Number of tables: 1
Supplementary material: 2

Abstract

Objective: To detect and quantify peripheral nerve lesions in multiple sclerosis (MS) by magnetic resonance neurography (MRN).

Methods: 36 patients diagnosed with MS based on the 2010 McDonald criteria (34 with the relapsing-remitting form, 2 with clinically isolated syndrome) with and without disease modifying treatment were compared to 35 healthy age/sex-matched volunteers. All patients underwent detailed neurological and electrophysiological examinations. 3T MRN with large anatomical coverage of both legs and the lumbosacral plexus was performed by using 2D fat-saturated, T2-weighted and dual echo turbo-spin-echo sequences as well as a 3D T2-weighted, fat-saturated SPACE sequence. Besides qualitative visual nerve assessment, a T2w-signal quantification was performed by calculation of proton-spin-density and T2-relaxation time. Nerve diameter was measured as a morphometric criterion.

Results:T2w-hyperintense nerve lesions were detectable in all MS patients with a mean lesion number at thigh level of 151.5±5.7 vs. 19.1±2.4 in controls ($p<0.0001$). Nerve proton-spin-density was higher in MS (tibial/peroneal: 371.8±7.7/368.9±8.2) vs. controls (tibial/peroneal: 266.0±11.0/276.8±9.7;$p<0.0001$). In contrast, T2-relaxation time was significantly higher in controls (tibial/peroneal:82.0±2.1/78.3±1.7) vs. MS (tibial/peroneal:64.3±1.0/61.2±0.9; $p<0.0001$). Proximal tibial and peroneal nerve caliber was higher in MS (tibial:52.4±2.1mm²; peroneal:25.4±1.3mm²) vs. controls (tibial:45.2±1.4mm²; $p<0.0015$; peroneal:21.3±0.7mm²; $p=0.0049$).

Interpretation: Peripheral nerve lesions could be visualized and quantified in MS *in vivo* by high resolution MRN. Lesions are defined by an increase of proton-spin-density and a decrease of T2-relaxation time, indicating changes in the microstructural organization of the extracellular matrix in peripheral nerve tissue in MS. By showing involvement of the peripheral nervous system in MS, this proof-of-concept study may offer new insights into the pathophysiology and treatment of MS.

Keywords:

Magnetic resonance neurography, multiple sclerosis, electrophysiology, peripheral nervous system, proton spin density

Introduction

Multiple sclerosis (MS), one of the most common acquired chronic neurological diseases, is traditionally regarded as restricted to the CNS, but the exact etiology is still unclear. With an estimated prevalence of 2 million affected people worldwide, it is one of the leading causes of disability in young adults.[1] The clinical presentation of MS is heterogeneous with sensory, motor, visual and autonomic symptoms.

Clinically, MS is diagnosed based on the principles of symptom dissemination in space and time as defined by the Poser criteria.[2] According to the 2010 McDonald criteria, the early diagnosis of MS after a single clinical event can be established by the radiological demonstration of lesion dissemination in space and time.[3]

Few studies, most of them case reports, suggest the concurrence of demyelination in the central nervous system (CNS) and peripheral nervous system (PNS) in MS. Earlier neuropathological reports described segmental demyelination, hypertrophic neuropathy and reduction in myelin thickness in few MS patients.[4,5] Large electrophysiological studies of nerve conduction abnormalities in MS are rare and documented results are inhomogeneous regarding type, frequency and extent of PNS involvement.[6,7]

High-resolution magnetic resonance neurography (MRN) enables early detection and precise localization of peripheral nerve lesions with high sensitivity, down to the level of nerve fascicles in various neuropathies, and thus can overcome typical diagnostic limitations of nerve conduction studies (NCS).[8,9] With an extensive MRN imaging protocol and in correlation with NCS, we 1) tested the involvement of the PNS in MS, 2) analyzed peripheral nerve lesions by *in vivo* visualization, localization and T2w-signal quantification, and 3) compared MRN findings of healthy volunteers to those of MS patients in correlation with the presence of spinal cord lesions.

Materials and methods

Study design and patients

The local ethics committee approved this study (University of Heidelberg S-405/2012; J.P., M.B.) and all participants gave written informed consent. 36 MS patients (21 female, 15 male, mean age 32.1 years, range 18-43, 2010 McDonald criteria fulfilled in all patients) with either relapsing-remitting MS (>3 years, range 3-13; n=34) or with clinically isolated syndrome

(n=2) and 35 sex and age matched healthy volunteers (19 female, 16 male, mean age 31.6, range 22-40), were included in this prospective, cross-sectional, single center study between May 2015 and September 2016. Current Gadolinium-enhanced MRI studies of the brain and spine were available in all patients with MS. The mean time gap between the acquisition of the MRN scans and the most recent available CNS MRI was 1.5±0.3 months (median = 1 month) for imaging of the brain and 5.5±1.3 months (median = 3 months) for imaging of the spinal cord. Overall exclusion criteria were, age <18 or >45, pregnancy, any contraindications for MRI, any risk factors for neuropathy such as diabetes mellitus, alcoholism, malignant or infectious diseases, any therapy with steroids in the eight weeks immediately prior to the MRI scans, and any previous exposure to neurotoxic agents. Additionally, by taking a detailed past medical history, any sensory or motor symptoms in the upper or lower extremities, any history of neuropathy, any previous spine surgery, and any permanent medication was ruled out in all healthy volunteers.

Clinical and electrophysiological examination

A detailed medical history was documented for each patient and a comprehensive neurological examination (R.D.; B.W.; M.K.K.) was performed, including evaluation of the Expanded Disability Status Scale.[10] NCS of the left leg included: distal motor latencies, compound muscle action potentials, and F-waves of the tibial and peroneal nerves, nerve conduction velocities of the tibial, peroneal and sural nerves, and sensory nerve action potentials of the sural nerve (M.W.). Skin temperature was controlled at a minimum of 32°C. Detailed clinical and electrophysiological data are presented in Table 1 and 2.

MRN protocol

All participants underwent high-resolution MRN in a 3.0 Tesla MR-scanner (Magnetom TIM-TRIO, Siemens Healthcare, Erlangen, Germany):

(1) 3D T2-weighted inversion recovery SPACE (Sampling Perfection with Application-optimized Contrasts using different flip angle Evolution) sequence for imaging of the lumbar plexus and spinal nerves with 50 axial reformations/patient: repetition time / effective echo time / inversion time 3000 / 62 / 210 ms, field of view 305 x 305 mm^2,

matrix size 320 x 320 x 104, slice thickness 1.0 mm, no gap, voxel size 1.0 x 1.0 x 1.0 mm^3, acquisition time 8:32 min.

(2) Axial high resolution T2-weighted turbo spin echo 2D-sequences with spectral fat-saturation (three slabs at the right leg). Slab 1: proximal thigh to mid-thigh; slab 2: lower leg with alignment of its proximal edge with the tibiofemoral joint space; slab 3: ankle level with alignment of the distal edge of the imaging slab on the tibiotalar joint space. Repetition time / echo time 5970 / 55 ms, field of view 150 x 150 mm^2, matrix size 512 x 512, slice thickness 3.5 mm, interslice gap 0.35 mm, voxel size 0.4 x 0.3 x 3.5 mm^3, 35 slices, acquisition time per slab 4:42 min.

(3) Axial high-resolution dual echo turbo spin echo 2D-sequence with spectral fat saturation (one slab per leg, equaling two slabs per subject): mid-thigh to distal thigh with alignment of the distal edge of this imaging-slab on the tibiofemoral joint space. Repetition time 5210 ms, echo $time_1$ / echo $time_2$ 12 / 73 ms, field of view 150 x 150 mm^2, matrix size 512 x 512, slice thickness 3.5 mm, interslice gap 0.35 mm, voxel size 0.4 x 0.3 x 3.5 mm^3, 35 slices, acquisition time per slab 7:30 min.

Net imaging time including survey scans was 38:02 min. Patient and coil repositioning required additional time, resulting in a total examination time of 60-70 min per participant. A 4-channel body-array flex-coil (Siemens Healthcare) was used for imaging of the lumbar plexus (sequence 1), and a 15-channel Transmit-Receive extremity-coil (INVIVO) for imaging of the right and left leg, respectively (sequence (2) and (3)). All coils used in this study are commercially available.

Image post-processing and statistical analysis

All images generated by MRI sequences (2) and (3) were pseudonymized (M.B.; J.P.) and subsequently analyzed in FSL, a dedicated software for neuroimaging data evaluation.[11] Tibial and peroneal fascicles of the sciatic nerve and their distal continuation as either tibial or peroneal nerve were manually segmented by one neuroradiologist (G.H.H.) from proximal thigh down to distal ankle level on 140 axial slices for the left leg, and only at thigh level on additional 35 slices for the right leg. The contour between nerve fascicles and the epineurium was used as a reliably visible segmentation border. Slice numbering for the tibial nerve was from 0 (most proximal slice at proximal thigh level) to 139 (most distal slice at ankle level) and from 0 to 60 (level of the fibular head) for the peroneal nerve. For simplification, we refer

to tibial fascicles of the sciatic nerve and corresponding tibial nerve as tibial nerve only, and to peroneal fascicles of the sciatic nerve and corresponding common peroneal nerve as peroneal nerve.

Qualitative evaluation of nerve lesions

Based on the 2010 McDonald criteria, the evaluation of T2w hyperintense lesions in the brain and spinal cord is an established method in the initial diagnostic work-up of patients with MS, as well as in their lifelong radiological follow up. According to this standard procedure, two experienced, independent neuroradiologists (J.J; J.K.) who were blinded to clinical data, performed a visual evaluation and determination of the total sciatic nerve lesion count on 20 representative axial imaging slices at left proximal thigh level. We defined a nerve lesion as a nerve fascicle with an abnormally high T2w signal. Lesion number per slice position was counted and then summed to a total lesion number within the imaged volume per participant. Subsequently, mean values were calculated over all participants within either the MS or the control group.

Recent spinal cord MRIs of all MS patients were additionally analyzed to exclude potential external sources of nerve affection such as spinal cord or nerve root compression due to herniated vertebral disks or spinal tumors. Once external reasons for nerve damage were ruled out, the total number of T2w hyperintense lesions to the spinal cord was evaluated. The total number of spinal cord lesions was then correlated with the total number of sciatic nerve lesions at thigh level.

Tibial and peroneal nerve T2w signal

In previous studies on nerve lesion detection and quantification in two different polyneuropathies,[12,13] we performed an extensive histogram based normalization of nerve T2w signal intensities and an fully-automatic and operator-independent binary classification of respective tibial and peroneal nerve voxels as either nerve lesion voxels or non-lesion voxels. With this method we have already proven, that an increase of nerve T2w signal reflects true nerve lesions.[12,13] To facilitate statistical evaluations, we analyzed nerve T2w signal without any further signal normalization in the current study.

Mean nerve T2w signal was calculated per slice position for each subject and for each left leg. To receive detailed information about the anatomical distribution of nerve lesions and thereby information about the location of predominant nerve affection, we compared mean tibial nerve T2w signals of 35 slices at proximal to mid-thigh level (slice positions 0-35) to its distal equivalent of 35 slices at the lower leg (proximal to middle part; slice positions 70-105). The peroneal nerve was evaluated from proximal to mid-thigh level (slice positions 0-35) only. Averaged mean values within all proximal slices were statistically compared between the two groups (MS versus controls) by using the Mann-Whitney test; additional mean values within all distal slices were evaluated for the tibial nerve only.

Nerve lesion quantification: apparent T2 relaxation time and proton-spin-density

Quantification of nerve lesions was performed by calculating the apparent T2 relaxation time ($T2_{app}$, Equation 1) and proton spin density (ρ, Equation 2), by the following formulas:[14]

1) $$T2_{app} = \frac{TE_2 - TE_1}{\ln(SI(TE_1)/SI(TE_2))}$$

2) $$\rho = \frac{SI(TE_1)}{\exp(-TE_1/T2_{app})}$$

As indicated by the two formulas, calculation of $T2_{app}$ and ρ required the acquisition of an additional pulse sequence at two different echo times (sequence (3) with echo $time_1$ = 12 ms and echo $time_2$ = 73 ms). To hold a reasonable total acquisition time, the dual echo sequence was acquired at thigh level only. That was done in accordance with previous studies in different neuropathies, where we have already proven their feasibility of application in the PNS, and their high sensitivity for early nerve lesion detection.[12 13]

Morphometric quantification: Nerve diameter

Nerve caliber was analyzed by measuring the complete cross sectional area of the tibial and peroneal nerve on each axial slice. Two-way ANOVA was performed to test group differences (MS versus controls) and differences between anatomical regions (proximal slice

positions 0-69 versus distal slice positions 70-139). Peroneal nerve caliber was analyzed from proximal thigh level down to the level of the fibular head only (slice positions 0-60).

Lumbosacral plexus and spinal nerves

Bilateral dorsal root ganglia and corresponding proximal spinal nerves L5 and S1 were segmented on axial reformations of sequence (1) by manually delineating the nerve circumference as the intraneural region of interest. In the same manner, the lumbosacral plexus was segmented at level of the sciatic notch on both sides. Subsequently, signal ratios between intraneural regions of interest and ipsilateral psoas (L5 and S1) or piriformis muscle (plexus) were calculated. Additional quantification of spinal nerve and plexus caliber was performed by measuring the cross sectional area of the corresponding nerve on each axial slice.

Statistical analysis

Statistical data analysis was performed with GraphPad Prism 6 (J.K; J.M.H.). Differences between MS patients and controls were evaluated with the Mann-Whitney test. Where appropriate, a one-way or two-way ANOVA was used for *a priori* assumptions, and subsequent post hoc comparisons were evaluated with the Fisher test. Statistical tests were two-tailed and an alpha-level of significance was defined at $p < 0.05$. All results are documented as mean values ± Standard Error of the Mean (SEM).

Results

Clinical and electrophysiological data

There was no significant difference between MS patients and controls for age, sex, body weight and height (Table 1). In MS patients, the mean overall EDSS score was 2.0 ± 0.3. 31 patients received disease-modifying medical treatment (EDSS 2.0 ± 0.3), while five patients had been free of immunomodulating medical treatment during the course of their disease (EDSS 2.1 ± 0.9). All patients fulfilled the revised 2010 McDonald criteria (Supplementary Table 1). Electrophysiological findings were normal with the exception of four patients having marginally amplitude-reduced sural sensory nerve action potentials (ID 11, 13, 15;

Supplementary Table 2), one patient having non-elicitable F-waves of the peroneal nerve (ID 23; Supplementary Table 2), and another one with non-elicitable F-waves of the tibial and peroneal nerves (ID 15; Supplementary Table 2) in otherwise normal electroneurographic parameters and without clinical evidence of peripheral nerve dysfunction (Supplementary Table 2). Moreover, there was no evidence for metabolic or vasculitic neuropathy in CSF- or blood tests (e.g. metabolic panel, vitamin B12) at the time of diagnosis. Lumbar MRI ruled out concurrent nerve root compression.

Qualitative evaluation of nerve lesions

Qualitative visual evaluation revealed marked T2w-hyperintense nerve lesions in all MS patients independent of their prior medication and with a mean lesion number at thigh level of 152.7 ± 4.1 versus 19.3 ± 1.7 in controls ($p < 0.0001$). Further subgroup analyses between treated MS patients versus controls and also between untreated MS patients versus controls revealed high differences for both groups ($p < 0.0001$; Fig 1 and 2), while differences between treated and untreated MS patients were not significant ($p = 0.64$). Calculated Cohens kappa was 1.000 for inter-observer reliability to visually classify all participants into either MS or non-MS. High inter-observer reliability was also found for the subsequent evaluation of the sciatic nerve lesion count (lesion number) with a Pearson´s r of 0.9978 (control group) and 0.9892 (MS group). Fascicular lesions in all MS patients showed a diffuse distribution pattern with a median length of 7.35 mm, not involving fascicular segments longer than 11.2 mm.

The additional evaluation of spinal cord T2w lesions in MS patients revealed a strong negative correlation between spinal cord lesions and sciatic nerve lesions ($r=-0.51$; $p=0.002$). In all MS patients we found no spinal cord T2w lesions below lumbar segment 1 (L1) and no signs of spinal cord or nerve root compression.

Proton spin density

The Mann-Whitney test revealed higher ρ in MS patients (tibial nerve: 371.8 ± 7.7; peroneal nerve: 368.9 ± 8.2 a.u.) versus healthy controls (tibial nerve: 266.0 ± 11.0; peroneal nerve: 276.8 ± 9.7 a.u.; $p < 0.0001$ for both nerves).

As ρ was found to be the parameter with highest sensitivity for detecting PNS affection in MS patients, and to rule out that an increase of ρ was not related to the appearance of spinal cord lesions, we evaluated ρ in subgroups of MS patients with and without spinal cord lesions. One-way ANOVA revealed marked differences between the three groups (MS patients with spinal cord lesions versus MS patients without spinal cord lesions versus controls) with $p < 0.0001$. Post-hoc comparisons showed significant differences of mean tibial nerve ρ between controls (26.0 ± 11.0 a.u.) versus MS with spinal cord lesions (368.0 ± 8.0 a.u.; $p < 0.0001$) and versus MS without spinal cord lesions (387.3 ± 21.9 a.u.; $p < 0.0001$; Fig 4), while differences between MS patients with and without spinal cord lesions were not significant ($p = 0.45$).

Apparent T2 relaxation time

Differences of $T2_{app}$ between MS patients and controls was highly significant ($p < 0.0001$ for both nerves), with higher T2app in controls (tibial nerve: 82.0 ± 2.1 ms; peroneal nerve: 78.3 ± 1.7 ms) compared to MS patients (tibial nerve: 64.3 ± 1.0 ms; peroneal nerve: 61.2 ± 0.9 ms).

Mean ρ and $T2_{app}$ are plotted for each group and nerve in Fig. 3.

Nerve T2w-signal

Proximal tibial and peroneal nerve T2w signal was not significantly different between MS patients (tibial nerve: 218.5 ± 6.3; peroneal nerve: 157.6 ± 4.6 a.u.) and controls (tibial nerve: 210.6 ± 7.5; $p = 0.40$; peroneal nerve: 148.3 ± 4.6 a.u.; $p = 0.12$). T2w signal of the distal tibial nerve was also not significantly different between MS patients (148.3 ± 5.1) and controls (153.8 ± 6.5 a.u.; $p = 0.55$). A significantly higher tibial nerve T2w signal could be observed at thigh level versus lower leg level in MS as well as in controls ($p < 0.0001$).

Morphometric quantification: Nerve diameter

Differences in proximal nerve caliber (measured as mean cross-sectional area) between MS patients and controls were significant at the level of the lumbosacral plexus and spinal nerves, (MS group: lumbosacral plexus 90.6 ± 4.8, spinal nerve L5 47.6 ± 1.9, spinal nerve S1 / 47.8

± 2.0 mm²; control group: lumbosacral plexus 34.3 ± 1.5, spinal nerve L5 16.4 ± 0.6, spinal nerve S1 13.2 ± 0.6 mm²; $p < 0.0001$ for all locations). Differences in proximal nerve caliber were also significant for the tibial nerve (MS group 52.4 ± 2.1 mm²; controls 45.2 ± 1.4 mm²; $p = 0.0015$) and the peroneal nerve (MS group 25.4 ± 1.3 mm²; controls 21.3 ± 0.7 mm²; $p = 0.0049$). However, distally, at lower leg level, there was no significant difference of tibial nerve caliber between MS patients (34.2 ± 1.8 mm²) and controls (32.1 ± 0.9 mm²; $p = 0.35$).

Discussion

To date, it is widely accepted that pathological changes in MS are restricted to the CNS and cranial nerves. This is reflected by the revised 2010 McDonald criteria which only consider cerebral or spinal cord inflammatory lesions. Moreover, electrophysiological tests are commonly negative for signs of PNS involvement in MS. However, in many patients suffering from MS, there is a large, yet inexplicable gap, between the severity of clinical symptoms and a comparably low burden of CNS lesions.[15,16] Few studies have indicated that damage might occur in parts of the PNS as well,[17,5,18,7] but to date, there is no solid proof of a distinct PNS affection *in vivo*.

To the best of our knowledge, our study is the first to prove an involvement of the PNS in MS patients by high-resolution MRN regardless of disease duration or medical treatment. Similar to the established diagnostic evaluation of T2w-hyperintense lesions in the brain and spinal cord, lesion number of the PNS can be determined visually by counting single T2w-hyperintense fascicles within lower extremity peripheral nerves with high inter-rater reliability (Fig. 1 and 2). Further signal quantification revealed a highly significant increase of ρ in MS patients compared to healthy controls, while $T2_{app}$ was significantly lower in the MS cohort (Fig. 3). Both, ρ and $T2_{app}$ contribute to the T2w signal. However, as defined by the T2 decay, which can be calculated according to the formula $S(TE)=\rho*\exp(-TE/T2app)$ (S=signal, TE=echo time), an overall T2w signal increase is possible when there is an increase in ρ or T2app, or the increase of one of the two parameters outweighs the decrease of the other. In our study cohort, the observed visual increase of fascicular T2w signal was mainly generated by an increase of ρ, which according to the T2 decay formula, outweighed the decrease of T2app with regards to the signal in the T2 weighted sequence.

The subsequent classification of PNS lesions as areas of elevated ρ and slightly reduced $T2_{app}$ suggests, that an increase in free-water protons, as one would expect in endoneural edema, is not the main underlying pathomechanism of PNS involvement in MS.[19,20] Instead, an increasing ρ indicates that damage to the PNS in MS is more likely induced by changes in the microstructural organization of the extracellular matrix as a consequence of an increase in plasma protein leakage through the endovascular barrier, and the pathogenesis of a pro-inflammatory milieu.[21] This mechanism was previously hypothesized as key factor in the pathomechanism of typical PNS diseases like amyloidotic or diabetic neuropathy.[12,13] Additionally, previous MRI studies focusing on changes of ρ in CNS lesions related to MS, found a clear correlation between an increased ρ and areas of demyelination in the brain and spinal cord,[22] suggesting that our findings represent a peripheral co-demyelination of the PNS in MS. Thus, an increase in ρ supports the assumption that PNS lesions or rather a peripheral co-demyelination is likely to be caused by immunologic reactions and destruction of molecules such as connexin 32 or myelin associated glycoproteins that are common to myelinating cells in both, the PNS and the CNS.[23,24,25]

Alterations of $T2_{app}$ in MS are still not fully understood.[26] Previous studies described an initial increase of $T2_{app}$ in acute MS lesions with a subsequent decrease in chronic lesions, but results are controversial.[27,28,29,30] One possible explanation might be a balance change of the total water pool, towards a higher amount of bound water and a lower amount of free water molecules, as it would be the case in the suggested hypotheses of an inflammatory process combined with an impairment of the blood nerve barrier, a pathologically high plasma protein leakage and an impairment of the lipid-rich myelin sheath. [1,21]

Peripheral nerve lesion detection by means of the described qualitative and quantitative analysis of the MR signal was further validated by an additional increase of proximal tibial and peroneal nerve caliber in MS, representing a pure morphometric MRN criterion for nerve impairment. This proximal nerve caliber increase might also point towards an inflammatory process, especially as it was associated with a higher PNS lesions number and an increased ρ. However, differences between MS patients and healthy controls were insignificant for distal tibial nerve caliber, suggesting a proximal predominance of PNS affection

This study is limited by the fact that most enrolled patients were under disease-modifying treatment. An argument could be made that lesions are attributed to secondary effects of MS

modifying medications rather than to the disease itself. To the contrary, we found no difference in the lesion number of patients with and without medication. Furthermore, MS patients were treated with a multitude of different immunomodulating drugs, of which none have known acute or chronic neurotoxic side effects. One might also argue that, in comparison to controversial results in previous studies, but also in the absence of positive electrophysiological examination results, our finding of an elevated number of PNS lesions in all included patients seem improbable. An explanation might be that PNS involvement is very subtle in many cases and thus may escape detection by regular NCV exams, as in our study. However, recent studies focusing on demyelinating processes in corneal fibers of the trigeminal nerve have shown that PNS demyelination is present in more patients than clinical symptoms might suggest.[31] Both, corneal fiber microscopy and MRN have already shown that damage to PNS fibers is detectable prior to the beginning of clinical symptoms.[12,31,32]

A potential factor that might contribute to the occurrence of PNS lesions might be that PNS lesions are the result of Wallerian degeneration caused by spinal cord lesions in MS.[9] Although we cannot fully exclude such secondary effects of CNS lesions, we found no differences in MRN markers between patients with and without spinal cord lesions (Fig. 4). The finding of a negative correlation between PNS lesions and spinal cord lesions and also the exclusion of any other potential sources of CNS damage in the additionally available spinal MRIs, makes it even more unlikely that the observed PNS lesions occur as a direct consequence of spinal cord lesions. Furthermore, the diffuse, non-focal PNS lesion distribution in our study cohort that involved only short continuous fascicular segments, points more towards an underlying inflammatory or demyelinating pathomechanism as one would expect in MS. In contrast, an involvement of longer fascicular segments or a somatotopic fascicular organization as it has been demonstrated in Wallerian degeneration,[33,34,35,36] could be excluded. Electrophysiological examinations also revealed no abnormalities due to an axonal loss, as they typically occur in Wallerian degeneration. For all these reasons, our study results indicate a potential occurrence of different antibodies in MS with and without CNS predominance.

Future studies should point at differences in patients with MS and clinically isolated syndrome with and without PNS lesions. Special attention should be paid to individuals with a relatively low CNS lesion burden in comparison to severe clinical symptoms, and to the influence of different disease modifying drugs on the development of PNS lesions.

In summary, this proof-of-concept study evidences PNS lesions in young MS patients *in vivo* by MRN with high structural resolution. The identification of PNS lesions suggests a peripheral co-demyelination, which may guide to a better understanding of discrepancies between clinical symptoms and CNS lesions detected by MRI. Most importantly it provides options for new pathophysiological concepts, and the identification of potential distinct immunoreactions targeting PNS antigens in MS with future implications on therapeutic approaches.

Acknowledgements

The study was supported in part by the German Research Foundation (SFB 1118 to S.H. and M.B., SFB 1158 to M.B.), the Amyloidosis Foundation (J.K.), and Alnylam Pharmaceuticals (J.K.).

R.D. was supported by the German Research Foundation (FOR 2289), S.H. by the Dietmar Hopp Foundation; B.W. by the German Ministry of Education and Research, the Dietmar Hopp Foundation, and Klaus Tschira Foundation; and M.B. by Siemens Healthcare, and the Dietmar Hopp Foundation.

We thank Mrs. Dorothea Willich (Department of Neuroradiology, Heidelberg University Hospital) for her ongoing support and excellent technical performance of all MRN examinations and Dr. Georges Sam (Department of Neurology, Heidelberg University Hospital) for excellent technical assistance in electrodiagnostics.

Author Contributions

J.K., G.H.H., J.J., J.P., M.P., and M.B. conceived and designed the study.

Acquisition and analysis of data were accomplished by J.K., G.H.H., J.J., R.D., M.W., S.H., B.W., M.K.K., and J.M.H.

J.K., G.H.H., J.J., W.W., and M.B. were responsible for writing and drafting a significant portion of the manuscript or figures.

Potential Conflicts of Interest

No conflicts to report.

References

1. Kister I, Bacon TE, Chamot E, et al. Natural history of multiple sclerosis symptoms. Int. J. MS Care 2013;15(3):146–58.
2. Poser CM, Paty DW, Scheinberg L, et al. New diagnostic criteria for multiple sclerosis: Guidelines for research protocols. Ann. Neurol. 1983;13(3):227–231.
3. Polman CH, Reingold SC, Banwell B, et al. Diagnostic criteria for multiple sclerosis: 2010 Revisions to the McDonald criteria. Ann. Neurol. 2011;69(2):292–302.
4. HASSON J, TERRY RD, ZIMMERMAN HM. Peripheral neuropathy in multiple sclerosis. Neurology 1958;8(7):503–10.
5. Pollock M, Calder C, Allpress S. Peripheral nerve abnormality in multiple sclerosis. Ann. Neurol. 1977;2(1):41–48.
6. Vogt J, Paul F, Aktas O, et al. Lower motor neuron loss in multiple sclerosis and experimental autoimmune encephalomyelitis. Ann. Neurol. 2009;66(3):310–322.
7. Anlar O, Tombul T, Kisli M. Peripheral sensory and motor abnormalities in patients with multiple sclerosis. Electromyogr. Clin. Neurophysiol. 2003;43(6):349–51.
8. Stoll G, Bendszus M, Perez J, Pham M. Magnetic resonance imaging of the peripheral nervous system. J. Neurol. 2009;256(7):1043–1051.
9. Bendszus M, Stoll G. Technology insight: visualizing peripheral nerve injury using MRI. Nat. Clin. Pract. Neurol. 2005;1(1):45–53.
10. Kurtzke JF. Rating neurologic impairment in multiple sclerosis: an expanded disability status scale (EDSS). Neurology 1983;33(11):1444–52.
11. Jenkinson M, Beckmann CF, Behrens TEJ, et al. FSL. Neuroimage 2012;62(2):782–90.
12. Kollmer J, Hund E, Hornung B, et al. In vivo detection of nerve injury in familial amyloid polyneuropathy by magnetic resonance neurography. Brain 2015;138(3):549–562.
13. Pham M, Oikonomou D, Hornung B, et al. Magnetic resonance neurography detects diabetic neuropathy early and with Proximal Predominance. Ann. Neurol. 2015;78(6):939–48.
14. Heiland S, Sartor K, Martin E, et al. In vivo monitoring of age-related changes in rat brain using quantitative diffusion magnetic resonance imaging and magnetic resonance relaxometry. Neurosci. Lett. 2002;334(3):157–60.
15. Rovaris M, Bozzali M, Santuccio G, et al. In vivo assessment of the brain and cervical cord pathology of patients with primary progressive multiple sclerosis. Brain 2001;124(Pt 12):2540–9.
16. Miller DH, Grossman RI, Reingold SC, McFarland HF. The Role of Magnetic Resonance Techniques in Understanding and Managing Multiple Sclerosis. Brain 1998;121 (Pt 1:3–24.
17. Schoene WC, Carpenter S, Behan PO, Geschwind N. “Onion bulb” formations in the central and peripheral nervous system in association with multiple sclerosis and hypertrophic polyneuropathy. Brain 1977;100(4):755–73.

18. Misawa S, Kuwabara S, Mori M, et al. Peripheral nerve demyelination in multiple sclerosis. Clin. Neurophysiol. 2008;119(8):1829–1833.

19. Abbas Z, Gras V, Möllenhoff K, et al. Analysis of proton-density bias corrections based on T_1 measurement for robust quantification of water content in the brain at 3 Tesla. Magn. Reson. Med. 2014;72(6):1735–1745.

20. Tofts PS, du Boulay EP. Towards quantitative measurements of relaxation times and other parameters in the brain. Neuroradiology 1990;32(5):407–15.

21. Davies G, Ramani A, Dalton C, et al. Preliminary magnetic resonance study of the macromolecular proton fraction in white matter: a potential marker of myelin? Mult. Scler. 2003;9(3):246–249.

22. Nijeholt GJ, Bergers E, Kamphorst W, et al. Post-mortem high-resolution MRI of the spinal cord in multiple sclerosis: a correlative study with conventional MRI, histopathology and clinical phenotype. Brain 2001;124(Pt 1):154–66.

23. Pichiecchio A, Bergamaschi R, Tavazzi E, et al. Bilateral trigeminal enhancement on magnetic resonance imaging in a patient with multiple sclerosis and trigeminal neuralgia. Mult Scler 2007;13(6):814–816.

24. Gartzen K, Katzarava Z, Diener H-C, Putzki N. Peripheral nervous system involvement in multiple sclerosis. Eur. J. Neurol. 2011;18(5):789–91.

25. Rovira A. Peripheral nervous system involvement in multiple sclerosis. Mult. Scler. J. 2017;23(5):751–751.

26. MacKay AL, Laule C. Magnetic Resonance of Myelin Water: An in vivo Marker for Myelin. Brain Plast. 2016;2(1):71–91.

27. Ormerod I, Bronstein A, Rudge P, et al. Magnetic resonance imaging in clinically isolated lesions of the brain stem. J. Neurol. Neurosurgery, Psychiatry 1986;49:737–743.

28. Goodkin DE, Rooney WD, Sloan R, et al. A serial study of new MS lesions and the white matter from which they arise. Neurology 1998;51(6):1689–97.

29. Larsson HB, Frederiksen J, Petersen J, et al. Assessment of demyelination, edema, and gliosis by in vivo determination of T1 and T2 in the brain of patients with acute attack of multiple sclerosis. Magn. Reson. Med. 1989;11(3):337–48.

30. Deoni SCL. Quantitative Relaxometry of the Brain. Top. Magn. Reson. Imaging 2010;21(2):101–113.

31. Mikolajczak J, Zimmermann H, Kheirkhah A, et al. Patients with multiple sclerosis demonstrate reduced subbasal corneal nerve fibre density. Mult. Scler. J. 2016;135245851667759.

32. Kollmer J, Sahm F, Hegenbart U, et al. Sural nerve injury in familial amyloid polyneuropathy: MR neurography vs clinicopathologic tools. Neurology. 2017;89(5):475-84.

33. Baumer P, Weiler M, Bendszus M, Pham M. Somatotopic fascicular organization of the human sciatic nerve demonstrated by MR neurography. Neurology 2015;84(17):1782–1787.

34. Hilgenfeld T, Jende J, Schwarz D, et al. Somatotopic Fascicular Lesions of the Brachial

Plexus Demonstrated by High-Resolution Magnetic Resonance Neurography. Invest. Radiol. 2017;1.

35. Bendszus M, Wessig C, Solymosi L, et al. MRI of peripheral nerve degeneration and regeneration: correlation with electrophysiology and histology. Exp. Neurol. 2004;188(1):171–177.

36. Stanisz GJ, Midha R, Munro CA, Henkelman RM. MR properties of rat sciatic nerve following trauma. Magn. Reson. Med. 2001;45(3):415–20.

Figure legend

Figure 1: MRN source images. Representative MRN of the left sciatic nerve at mid-thigh level (high-resolution T2-weighted turbo spin echo sequence with spectral fat-saturation, 3T) in **(A)** a healthy control subject, **(B)** a patient with MS without disease modifying treatment and **(C)** a MS patient under disease modifying treatment. A high lesion number, measured as a marked T2w-hyperintensity in a multitude of sciatic nerve fascicles can be seen in MS patients without **(B)** and with **(C)** disease modifying treatment. Normal sciatic nerve T2w signal in a representative healthy control **(A)**.

Figure 2: Total sciatic nerve T2w lesion count. Mean values of the visually evaluated total nerve lesion number plotted for MS patients under immunomodulatory therapy (MS treated), MS patients without any current or previous immunomodulatory therapy (MS untreated), and controls. While differences between treated and untreated MS patients were not significant ($p=0.64$), differences between controls and each of the two MS subgroups were highly significant ($p<0.0001$).

Figure 3: Quantitative MRN markers of nerve T2w signal. Mean values of tibial (left) and peroneal (right) proton spin density **(A, B)** and apparent T2 relaxation time **(C, D)** are plotted for MS patients and controls. Proton spin density of the tibial **(A)** and peroneal nerves **(B)** was significantly higher in MS patients versus healthy controls ($p<0.0001$). In contrast, tibial (**C**) and peroneal (**D**) apparent T2 relaxation time was significantly higher in controls versus MS patients ($p<0.0001$).

Figure 4: Proton spin density. Mean values of tibial nerve proton spin density are plotted for MS patients with and without spinal cord T2w lesions and for controls. Note that differences in proton spin density between MS patients with and without T2w lesions to the spinal cord were not significant ($p=0.45$), while differences between controls and either MS subgroup were remarkable ($p<0.0001$).

Table 1: Demographic, clinical, radiological and electrophysiological data

Parameter	MS patients	Controls	p value
Age	32.1 ± 1.0	31.6 ± 1.3	0.25 (ns)
Sex (M/F)	15/21	16/19	n.a.
Body weight (kg)	73.6 ± 3.0	66.2 ± 1.5	0.10 (ns)
Height (cm)	179.1 ± 3.6	175.9 ± 2.2	0.49 (ns)
MS duration (months)	81.9 ± 7.3	n.a.	n.a.
Relapsing-remitting MS	34	n.a.	n.a.
Clinically isolated syndrome	2	n.a.	n.a.
Tibial nerve caliber (mm^2)	52.4 ± 2.1	45.2 ± 1.4	0.0015 (**)
Peroneal nerve caliber (mm^2)	25.4 ± 1.3	21.3 ± 0.7	0.0049 (**)
Total sciatic nerve T2w lesion number	152.7 ± 4.1	19.3 ± 1.7	<0.0001 (***)
ρ tibial nerve	371.8 ± 7.7	266.0 ± 11.0	<0.0001 (***)
ρ peroneal nerve	368.9 ± 8.2	276.8 ± 9.7	<0.0001 (***)
Total CNS T2w lesions	27.9 ± 3.9	n.a.	n.a.
Cerebral T2w lesions	25.9 ± 3.7	n.a.	n.a.
Spinal T2w lesions	2.0 ± 0.4	n.a.	n.a.
CNS lesions with contrast enhancement	3	n.a.	n.a.
Tibial nerve CMAP [mV]	21.1 ± 1.4	n.a.	n.a.
Tibial nerve NCV [m/s]	54 ± 1	n.a.	n.a.
Tibial nerve F-wave [ms]	48.9 ± 0.6	n.a.	n.a.
Tibial nerve DML [ms]	3.6 ± 0.1	n.a.	n.a.
Peroneal nerve CMAP [mV]	7.7 ± 0.8	n.a.	n.a.
Peroneal nerve NCV [m/s]	50 ± 1	n.a.	n.a.
Peroneal nerve F-wave [ms]	46.2 ± 0.7	n.a.	n.a.
Peroneal nerve DML [ms]	3.7 ± 0.1	n.a.	n.a.
Sural nerve SNAP [µV]	14.0 ± 1.4	n.a.	n.a.
Sural nerve NCV [m/s]	57 ± 1	n.a.	n.a.

DML = distal motor latency; CMAP = compound muscle action potential; NCV = nerve conduction velocity; SNAP = sensory nerve action potential; ns = not significant, ** = significant, *** = highly significant

MRN source images. Representative MRN of the left sciatic nerve at mid-thigh level (high-resolution T2-weighted turbo spin echo sequence with spectral fat-saturation, 3T) in (A) a healthy control subject, (B) a patient with MS without disease modifying treatment and (C) a MS patient under disease modifying treatment. A high lesion number, measured as a marked T2w-hyperintensity in a multitude of sciatic nerve fascicles can be seen in MS patients without (B) and with (C) disease modifying treatment. Normal sciatic nerve T2w signal in a representative healthy control (A).

80x240mm (300 x 300 DPI)

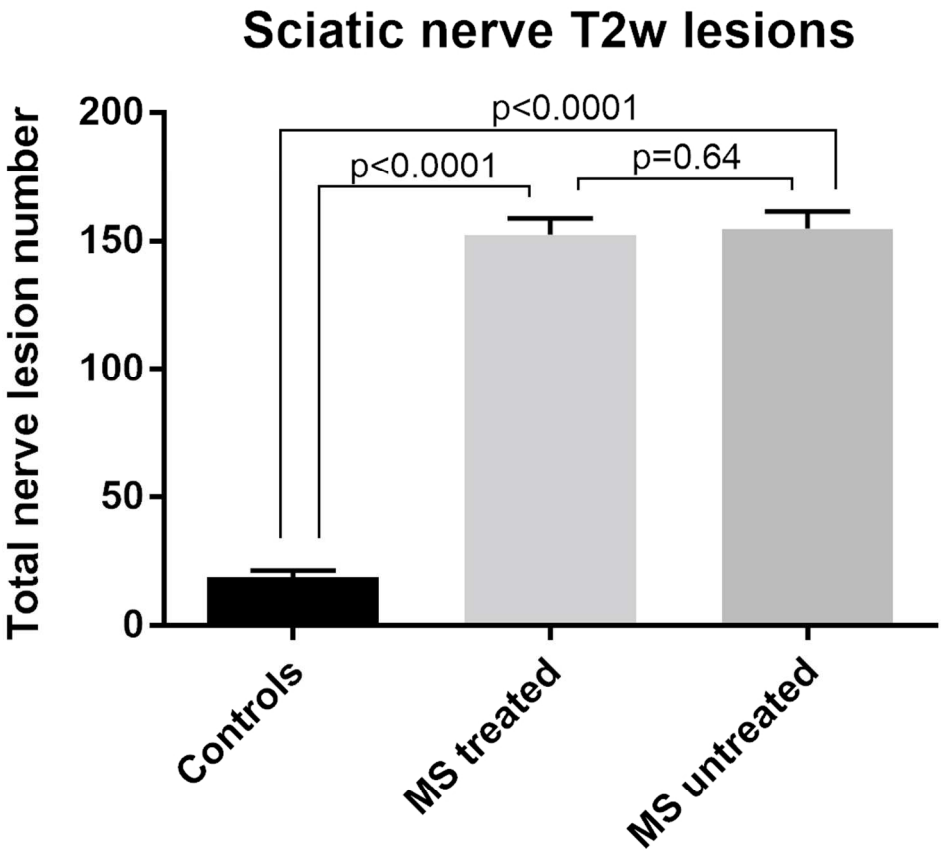

Total sciatic nerve T2w lesion count. Mean values of the visually evaluated total nerve lesion number plotted for MS patients under immunomodulatory therapy (MS treated), MS patients without any current or previous immunomodulatory therapy (MS untreated), and controls. While differences between treated and untreated MS patients were not significant (p=0.64), differences between controls and each of the two MS subgroups were highly significant (p<0.0001).

98x91mm (300 x 300 DPI)

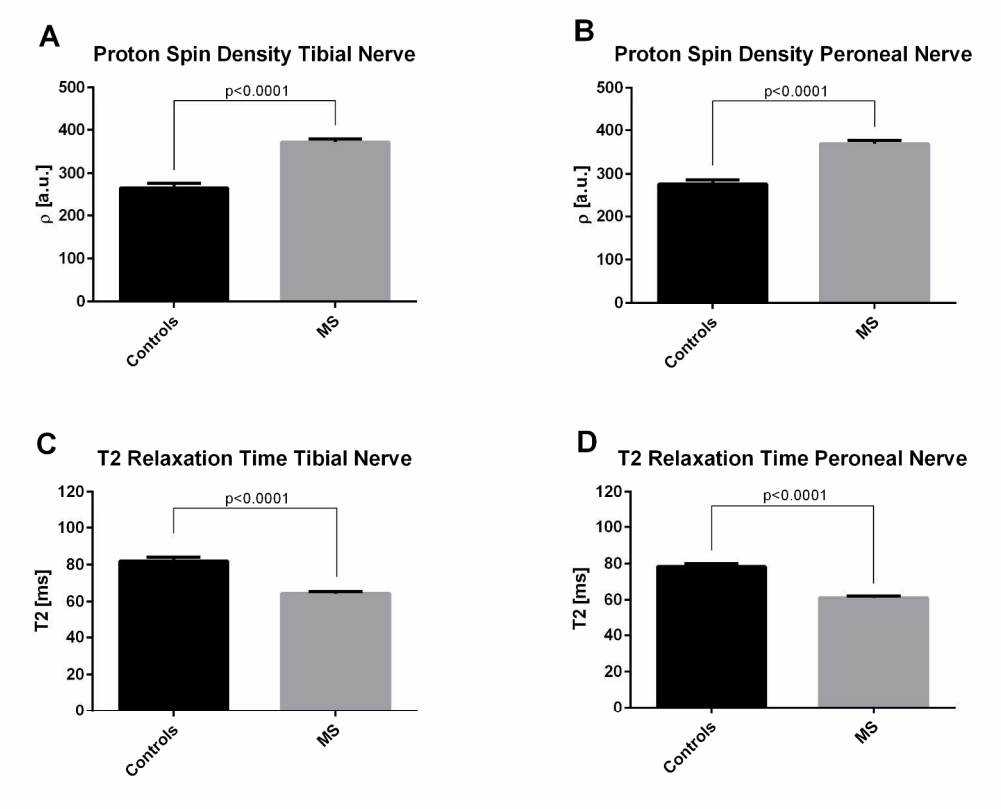

Quantitative MRN markers of nerve T2w signal. Mean values of tibial (left) and peroneal (right) proton spin density (A, B) and apparent T2 relaxation time (C, D) are plotted for MS patients and controls. Proton spin density of the tibial (A) and peroneal nerves (B) was significantly higher in MS patients versus healthy controls ($p<0.0001$). In contrast, tibial (C) and peroneal (D) apparent T2 relaxation time was significantly higher in controls versus MS patients ($p<0.0001$).

238x193mm (300 x 300 DPI)

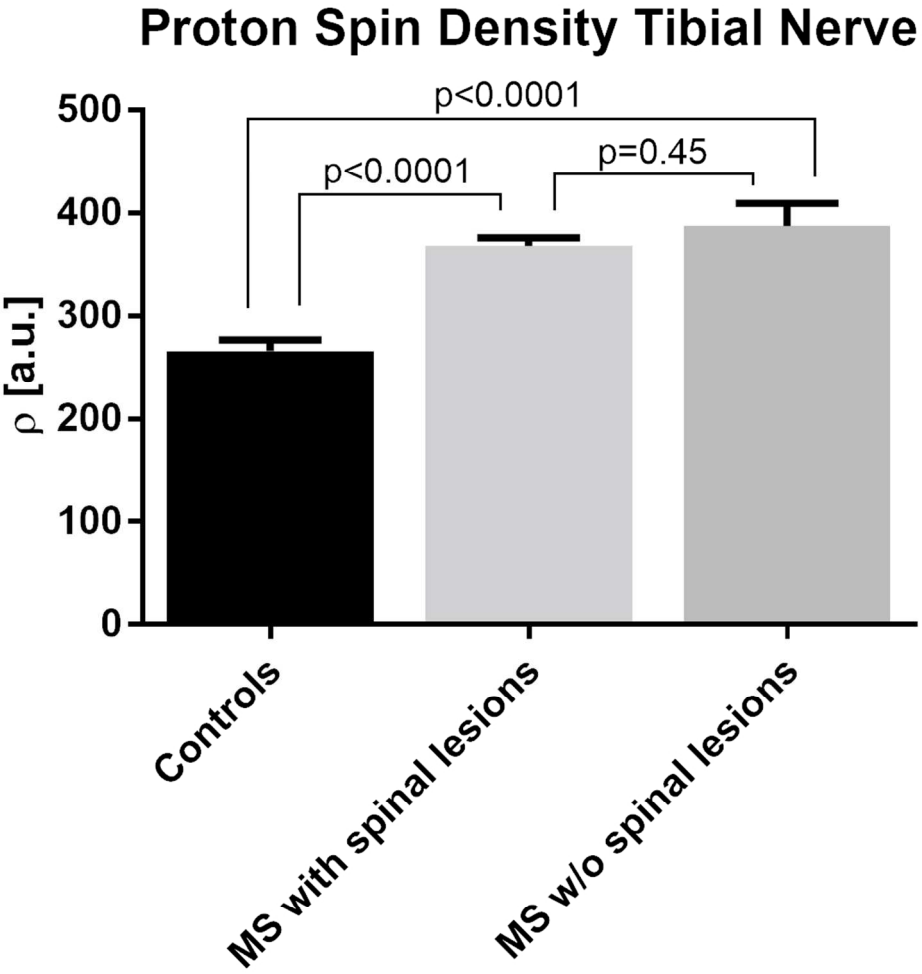

Proton spin density. Mean values of tibial nerve proton spin density are plotted for MS patients with and without spinal cord T2w lesions and for controls. Note that differences in proton spin density between MS patients with and without T2w lesions to the spinal cord were not significant (p=0.45), while differences between controls and either MS subgroup were remarkable (p<0.0001).

98x103mm (300 x 300 DPI)

Supplementary Table 1. Individual neurological deficits, EDSS scoring and current medications in MS patients

ID	Age/Sex	EDSS	Current neurologic examination findings	Current medication
1	33/F	4	Sensory: lower extremities	Natalizumab
2	36/F	2	Sensory: lower extremities	Dimethyl fumarate
3	30/M	0	Normal	Interferon beta-1a
4	39/F	1,5	Sensory: lower extremities	Interferon beta-1a
5	27/F	2	Sensory: lower extremities Cranial nerves	Fingolimod
6	30/M	3	Motoric: lower extremities Sensory: lower extremities	Dimethyl fumarate
7	34/F	3	Motoric: lower extremities Sensory: lower extremities	Interferon beta-1a
8	38/F	3,5	Sensory: lower extremities Autonomic nervous system	No medication
9	35/M	1,5	Normal	Dimethyl fumarate
10	39/M	3	Sensory: upper and lower extremities Motoric: upper and lower extremities Cranial nerves	No medication
11	31/M	0	Normal	Fingolimod
12	22/F	3	Sensory: upper and lower extremities	Fingolimod
13	36/M	0	Normal	Dimethyl fumarate
14	35/M	0	Normal	Fingolimod
15	39/M	4	Motoric: upper and lower extremities Sensory: upper and lower extremities	Dimethyl fumarate
16	27/F	4	Motoric: lower extremities	Natalizumab

			Sensory: lower extremities	
17	21/F	1,5	Sensory: upper extremities	Fingolimod
18	34/F	0	Normal	Fingolimod
19	35/M	6,5	Motoric: upper and lower extremities Sensory: upper and lower extremities Cranial nerves Autonomic nervous system	Natalizumab
20	40/M	2	Autonomic nervous system	Natalizumab
21	40/F	2	Sensory: upper and lower extremities	Natalizumab
22	25/F	0	Normal	Fingolimod
23	18/F	3,5	Motoric: upper and lower extremities Sensory: upper and lower extremities Autonomic nervous system	Alemtuzumab
24	28/F	2,5	Sensory: upper extremities Autonomic nervous system	Fingolimod
25	28/F	3,5	Motoric: lower extremities Sensory: upper and lower extremities Autonomic nervous system	Alemtuzumab
26	25/F	2,5	Motoric: upper and lower extremities Sensory: upper and lower extremities Cranial nerves	Alemtuzumab
27	39/M	2,5	Motoric: lower extremities	Fingolimod
28	35/M	0	Motoric: lower extremities Autonomic nervous system	Dimethyl fumarate
29	27/F	1	Motoric: lower extremities	Fingolimod
30	31/F	3,5	Motoric: upper and lower extremities Sensory: upper and lower extremities Cranial nerves	Fingolimod

31	24/F	0	Sensory: upper and lower extremities	Dimethyl fumarate
32	38/F	2	Motoric: upper extremities Sensory: upper and lower extremities	Natalizumab
33	36/M	2	Motoric: upper and lower extremities Sensory: lower extremities Cranial nerves	Alemtuzumab
34	28/F	0	Motoric: lower extremities	No medication
35	43/M	4	Motoric: lower extremities Autonomic nervous system	No medication
36	31/M	0	Normal	No medication

Sensory = sensory dysfunction / symptoms; motoric = motoric dysfunction / symptoms

Supplementary Table 2. Individual electrophysiological study results in MS patients

ID	Tibial nerve motor conduction study				Peroneal nerve motor conduction study				Sural nerve sensory conduction study	
No.	DML [ms]	CMAP [mV]	NCV [m/s]	F-wave [ms]	DML [ms]	CMAP [mV]	NCV [m/s]	F-wave [ms]	SNAP [μV]	NCV [m/s]
1	3.0 (N)	15.2 (N)	56 (N)	47.8 (N)	3.4 (N)	4.5 (N)	52 (N)	45.1 (N)	12.2 (N)	63 (N)
2	4.1 (N)	21.6 (N)	59 (N)	45.7 (N)	3.6 (N)	8.6 (N)	52 (N)	42.1 (N)	19.4 (N)	52 (N)
3	3.8 (N)	21.3 (N)	51 (N)	52.0 (N)	3.5 (N)	13.3 (N)	47 (N)	46,2 (N)	18.3 (N)	54 (N)
4	3.2 (N)	24.0 (N)	55 (N)	45.9 (N)	3.0 (N)	7.6 (N)	52 (N)	42.2 (N)	14.9 (N)	55 (N)
5	3.3 (N)	24.2 (N)	51 (N)	47.6 (N)	3.6 (N)	11.7 (N)	50 (N)	46.5 (N)	12.1 (N)	62 (N)
6	2.7 (N)	14.1 (N)	54 (N)	N/A	4.1 (N)	6.3 (N)	48 (N)	48.4 (N)	11.3 (N)	60 (N)
7	3.8 (N)	29.1 (N)	51 (N)	43.7 (N)	3.0 (N)	7.4 (N)	58 (N)	40.7 (N)	22.2 (N)	59 (N)
8	4.9 (N)	17.6 (N)	67 (N)	48.7 (N)	3.1 (N)	6.0 (N)	48 (N)	44.8 (N)	22.6 (N)	60 (N)
9	3.8 (N)	24.5 (N)	53 (N)	48.1 (N)	4.2 (N)	17.0 (N)	50 (N)	45.9 (N)	27.9 (N)	61 (N)
10	3.2 (N)	25.2 (N)	52 (N)	49.7 (N)	3.4 (N)	6.1 (N)	48 (N)	48.1 (N)	10.1 (N)	58 (N)
11	4.4 (N)	23.7 (N)	53 (N)	51.7 (N)	3.9 (N)	6.5 (N)	51 (N)	48.4 (N)	6.3 (P)	52 (N)
12	3.3 (N)	30.4 (N)	55 (N)	50.1 (N)	3.4 (N)	5.3 (N)	51 (N)	47.6 (N)	10.3 (N)	58 (N)
13	3.2 (N)	25.2 (N)	55 (N)	51.1 (N)	3.8 (N)	12.7 (N)	51 (N)	48.6 (N)	6.9 (P)	59 (N)
14	3.3 (N)	28.9 (N)	50 (N)	51.1 (N)	4.4 (N)	5.1 (N)	47 (N)	49.9 (N)	11.5 (N)	59 (N)
15	3.6 (N)	7.1 (N)	44 (N)	Absent (P)	3.8 (N)	4.9 (N)	41 (N)	Absent (P)	5.0 (P)	58 (N)
16	4.1 (N)	22.3 (N)	59 (N)	47,3 (N)	3.2 (N)	8.0 (N)	54 (N)	40.3 (N)	21.1 (N)	58 (N)
17	4.0 (N)	12.3 (N)	51 (N)	49.4 (N)	4.9 (N)	4.8 (N)	46 (N)	51.4 (N)	13.7 (N)	48 (N)
18	3.0 (N)	19.3 (N)	52 (N)	46.3 (N)	3.1 (N)	4.1 (N)	51 (N)	43.2 (N)	11.7 (N)	55 (N)

19	5.0 (N)	13.1 (N)	54 (N)	54.7 (N)	4.4 (N)	4.7 (N)	49 (N)	49.8 (N)	10.0 (N)	48 (N)
20	3.2 (N)	22.0 (N)	49 (N)	49.8 (N)	4.0 (N)	8.7 (N)	50 (N)	48.0 (N)	11.6 (N)	56 (N)
21	3.5 (N)	33.6 (N)	53 (N)	47.7 (N)	3.5 (N)	5.5 (N)	51 (N)	45.7 (N)	15.6 (N)	55 (N)
22	3.1 (N)	35.5 (N)	61 (N)	43.3 (N)	3.3 (N)	8.5 (N)	57 (N)	40.9 (N)	22.4 (N)	59 (N)
23	4.6 (N)	33.9 (N)	49 (N)	44.7 (N)	3.6 (N)	6.1 (N)	48 (N)	Absent (P)	11.7 (N)	49 (N)
24	5.0 (N)	13.6 (N)	45 (N)	54.6 (N)	4.0 (N)	10.5 (N)	44 (N)	49.0 (N)	14.6 (N)	54 (N)
25	3.3 (N)	23.5 (N)	53 (N)	48.0 (N)	4.3 (N)	5.4 (N)	49 (N)	48.0 (N)	14.8 (N)	55 (N)
26	4.0 (N)	24.1 (N)	49 (N)	52.9 (N)	4.3 (N)	8.3 (N)	50 (N)	48.9 (N)	10.6 (N)	51 (N)
27	3.9 (N)	16.1 (N)	53 (N)	52.8 (N)	4.2 (N)	5.0 (N)	45 (N)	53.2 (N)	12.3 (N)	61 (N)
28	4.3 (N)	19.4 (N)	55 (N)	51.7 (N)	4.7 (N)	9.2 (N)	51 (N)	48.7 (N)	14.7 (N)	50 (N)
29	3.2 (N)	19.4 (N)	51 (N)	48.4 (N)	3.9 (N)	10.0 (N)	49 (N)	45.1 (N)	12.6 (N)	57 (N)
30	3.0 (N)	33.7 (N)	54 (N)	44.8 (N)	3.9 (N)	5.4 (N)	50 (N)	42.7 (N)	17.4 (N)	63 (N)
31	3.1 (N)	28.2 (N)	51 (N)	49.0 (N)	4.1 (N)	11.4 (N)	48 (N)	42.9 (N)	13.0 (N)	59 (N)
32	3.4 (N)	22.4 (N)	61 (N)	42.6 (N)	3.4 (N)	9.8 (N)	51 (N)	41.5 (N)	18.0 (N)	66 (N)
33	3.4 (N)	30.7 (N)	52 (N)	49.2 (N)	3.9 (N)	6.5 (N)	49 (N)	46.2 (N)	13.6 (N)	55 (N)
34	3.2 (N)	28.0 (N)	50 (N)	43.0 (N)	4.1 (N)	8.0 (N)	57 (N)	44.0 (N)	15.1 (N)	66 (N)
35	3.8 (N)	26.0 (N)	49 (N)	51.0 (N)	4.0 (N)	9.2 (N)	49 (N)	48.0 (N)	8.7 (P)	50 (N)
36	2.9 (N)	24.7 (N)	53 (N)	53.0 (N)	4.4 (N)	8.4 (N)	54 (N)	48.0 (N)	18.5 (N)	46 (N)

DML = distal motor latency; CMAP = compound muscle action potential; NCV = nerve conduction velocity; SNAP = sensory nerve action potential; N = normal; P = pathological